Extended-Optimal-Power-Flow-Based Hierarchical Control for Islanded AC Microgrids

Tinajero, Gibran David Agundis; Aldana, Nelson Leonardo Diaz; Luna, Adriana Carolina; Segundo-Ramirez, Juan; Visairo, Nancy; Guerrero, Josep M.; Vasquez, Juan

Published in:
IEEE Transactions on Power Electronics

DOI (link to publication from Publisher):
10.1109/TPEL.2018.2813980

Publication date:
2019

Document Version
Accepted author manuscript, peer reviewed version

This article has been accepted for publication in a future issue of this journal, but has not been fully edited. Content may change prior to final publication. Citation information: DOI 10.1109/TPEL.2018.2813980, IEEE Transactions on Power Electronics

Extended OPF-Based Hierarchical Control for Islanded AC Microgrids

Gibran Agundis-Tinajero, Nelson L. Diaz, Adriana C. Luna, Juan Segundo-Ramírez, *Member, IEEE,* Nancy Visairo-Cruz, *Member, IEEE,* Josep M. Guerrero, *Fellow, IEEE*, Juan C. Vazquez, *Member, IEEE.*

***Abstract*—This paper presents the application of a hierarchical control scheme for islanded AC microgrids with a primary droop control and a centralized extended optimal power flow control. The centralized control is responsible for computing and sending, in an online manner, the control references to the primary controls in order to achieve three operational goals, i.e., improvement of the global efficiency, voltage regulation through reactive power management and compliance of the restrictions regarding the generation units capacities. Two case studies are defined and online tested in a laboratory-scaled microgrid implemented in the Microgrid Laboratory at Aalborg University. The primary controllers are included in a real-time simulation platform (dSPACE 1006), while the extended optimal power flow is conducted in a central controller by using a Smart Meter and LabVIEW for data acquisition and MATLAB for its implementation, taking into account load and capacity profiles. The obtained results show the reliability of the proposed scheme in a real system and its advantages over the conventional droop control.**

***Index Terms*—Hierarchical control, droop characteristics, islanded, microgrid, optimization, power flow, steady-state solution.**

I. Introduction

NOWADAYS the microgrid concept is taking an important role in enabling the integration of different distributed generation (DG) technologies, including renewable energy sources. The increasing integration of DG has meant a modernization of current electric power system by providing more reliability and sustainability [1]–[3]. However, due to the distributed operation of the generation units, new technical challenges have emerged mainly related to the voltage quality along the feeders and the proper power sharing considering the capacity and characteristics of the DG units [4], [5].

As a matter of fact, islanded microgrids represent an additional challenge since the DGs should perform a multifunctional operation. Apart from supplying power and ensuring the local demand, they should participate actively in the regulation of the islanded power system [6]. Several authors have addressed these challenges by developing different variants of primary controllers for achieving the power-sharing function between DGs [7]. Particularly, the droop-based methods have been widely used in the literature due to their characteristics and advantages, such as high flexibility, reliability, and capability of managing active and reactive power sharing by relying only on local measurements without the use of additional communication among DG units [8], [9].

Commonly, the DGs are interconnected through long radial feeders since they are usually far from the load location. However, due to the line impedance between DGs, serious problems appear related to power losses, reactive power flow and voltage quality along the feeders [5], [10], [11]. This kind of problems cannot be solved directly by the primary controllers, which require the support of complex control schemes for enhancing the operational characteristics required in the microgrids by providing power flow control and voltage regulation along the feeders [7], [9]. Hence, to cope with this problem, hierarchical multilevel controls have been proposed in the literature [7], [12]–[16].

In this regard, [12] presents a hierarchical control scheme for droop based AC microgrids, mainly focused on decentralized control for frequency regulation and active power management but not for reactive power requirements. A hierarchical control for AC and DC microgrids is shown in [13]. In this contribution, a coordination strategy to ensure the active power exchange is addressed. Additionally, the frequency and buses voltage are maintained at rated values. Nevertheless, only the active power management is addressed and lines impedance between the DG units are neglected. A hierarchical control including power flow optimization is presented in [14], the authors minimize losses and ensure a system frequency close to the nominal, leading to a frequency-stable operation of the islanded microgrid; the optimization is made offline and simulation case studies are presented. In [15], an optimal power flow based on glow-worm swarm optimization for islanded microgrids is presented, the power flow method includes unbalanced systems, and the optimization includes losses reduction and frequency constrains; the optimization objectives are achieved but the authors conclude that a reduction of computational time is needed for this approach. Recently, in [16], a multilayer scheme for active power management and voltage control with an optimization stage for cost minimization is presented; the control is validated through simulation results.

Note that, in the previous literature different mathematical methods and hierarchical schemes for the power flow based optimized operation of islanded microgrids have been addressed; however, offline schemes without experimental validation are presented. In this way, laboratory implementations are needed to validate that in practical environments, the pro-

G. Agundis, J. Segundo and N. Visairo are with the Universidad Autónoma de San Luis Potosí, San Luis Potosí, S.L.P., México.

A. Luna, J. Guerrero, and J. Vazquez are with the Department of Energy Technology, Aalborg University, Aalborg, 9220 Denmark.

N. L. Diaz is with the Engineering Faculty, Universidad Distrital F.J.C., Bogota 110231, Colombia (e-mail: nldiaza@udistrital.edu.co).

This article has been accepted for publication in a future issue of this journal, but has not been fully edited. Content may change prior to final publication. Citation information: DOI 10.1109/TPEL.2018.2813980, IEEE Transactions on Power Electronics

posed approaches have a close performance as in simulation stages even with system characteristics that were not modeled in the design stage.

Regarding the aforementioned, this paper presents a laboratory-scale evaluation of an optimal power flow as a hierarchical control for the online operation of islanded microgrids, additionally, in order to emulate practical situations encountered in islanded microgrids and to test the online optimization included in the hierarchical control, the case studies include random load profiles, random capacity profiles, efficiency curves for the conversion units, and the use of practical measurement instruments (smart meters) for the control action, showing the challenges, advantages and drawbacks of the proposed control scheme. Furthermore, in order to give a self-content work which can be able to be reproduced, the paper presents a detailed description of the controls, parameters, the equipment and software used for the implementation. On the other hand, it is important to mention that in this contribution, the optimization is made online and is activated when changes in the loads or the generation capacities occur, allowing an optimal operational performance for unpredicted loads or generation capacities changes in the islanded microgrid.

This paper proposes a hierarchical control scheme which includes a primary conventional droop control and a centralized extended optimal power flow (EOPF) control which is responsible of the active and reactive power sharing management. The online optimization is based, but not limited, on three operational objectives, i.e., efficiency improvement, voltage regulation and generation capacity constrains for the DG units. It is important to notice that, unlike the control schemes which incorporate the power flow for power sharing [9], in the proposed hierarchical scheme, the control dynamics of each DG unit are taken into account by including the droop characteristics in the conventional power flow formulation. In this way, the optimization of the droop characteristic coefficients and voltage references of the primary DG unit controls can be performed in order to achieve the operational objectives.

Please notice that, the proposed hierarchical control scheme can perform active and reactive power sharing and voltage regulation of several buses taking into account frequency variations, transmission lines impedance, capacities of the DG units. Additionally, since the control scheme is based on the extended optimal power flow, it is not limited to a specific islanded microgrid topology, therefore, it can be easily modified in the EOPF control stage.

This paper is organized as follows: Section II presents a detailed explanation of the proposed hierarchical control scheme, including the primary control, the extended power flow formulation and the optimization model. In Section III, the microgrid which is used as the test system and its laboratory implementation are shown. In Section IV, two case studies are addressed to show the reliability and advantages of the proposed control. Finally, in Section V, the conclusions of this work are discussed.

II. Proposed EOPF hierarchical control

Under islanded operation, at least one of the DG has to assume the responsibility of forming and ensuring the power balance in the islanded power system. This role may be assumed simultaneously by several DGs operating as grid-forming units in a multi-master configuration using droop control loops [17], [18]. The level of contribution of each DG in the power balance of the islanded system is defined following the frequency/active power (P-ω) and voltage/reactive power (Q-V) droop characteristics, which can be expressed as [19],

$$\omega = \omega^* - K_n^p P_n \tag{1}$$

$$V_n = V_n^* - K_n^q Q_n \tag{2}$$

where, ω^* is the nominal angular frequency of the system, V_n^* is the voltage amplitude reference of each n-th DG unit, K_n^p and K_n^q are the (P-ω) and (Q-V) droop coefficients, respectively [19]. The droop characteristics are defined by the aforementioned parameters as shown in Fig. 1. In accordance to the active and reactive power demand, the droop characteristics will determine the resultant angular frequency of the islanded power system (ω) and the voltage (V_n) of each DG unit, which as mentioned above, determine the proportion of active and reactive power shared by each DG. In this sense, it is possible to define the steady-state operation of each DG by adjusting the parameters of the droop characteristics.

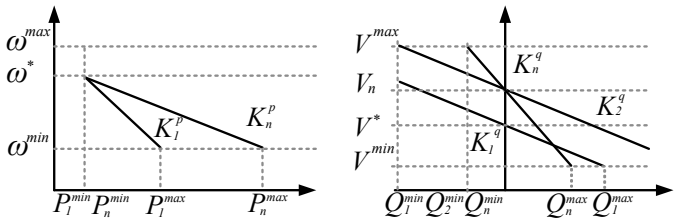

Fig. 1. Conventional droop characteristics [19].

Commonly, the DG are integrated through feeders since the energy sources may be located away from the load centers and points of common coupling (PCCs) as shown in Fig. 2 [20]. In this way, the reactive power sharing is affected by the line impedance along feeders [21], [22]. Additionally, the voltage quality at the PCCs and load centers may be compromised due to the effect of the (Q-V) droop control loops, and the voltage drop across the line impedance. On the other hand, the (P-ω) droop control can achieve an accurate active power sharing [23]; however, the total power contribution of each DG may be determined by the rated power of each energy resource.

On top of that, heterogeneous energy resources may require conversion stages of different characteristics in order to enable the integration of the primary energy resource to the power AC grid. This fact means different efficiencies in the conversion process, which should be also considered for defining the power contribution of each DG in order to enhance the global efficiency of the islanded microgrid [24].

Regarding the aforementioned, the proposed EOPF hierarchical control has the purpose of managing the active and

This article has been accepted for publication in a future issue of this journal, but has not been fully edited. Content may change prior to final publication. Citation information: DOI 10.1109/TPEL.2018.2813980, IEEE Transactions on Power Electronics

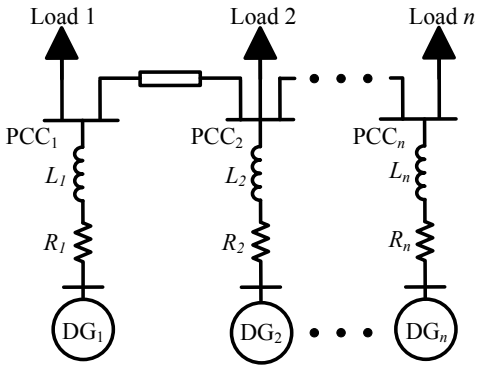

Fig. 2. Single line diagram of a microgrid with multiple feeders.

reactive power sharing, to achieve the specific operational goals of the islanded microgrid, such as:

- Maximize the global efficiency of the microgrid.
- PCC voltage regulation.
- Maintain the active and reactive power supplied by the DG units within its capacities.

These goals are reached through the optimal selection of the droop characteristic coefficients K_n^p and K_n^q, and voltage references of each DG unit in accordance to (1) and (2), which are included in an extended power flow formulation.

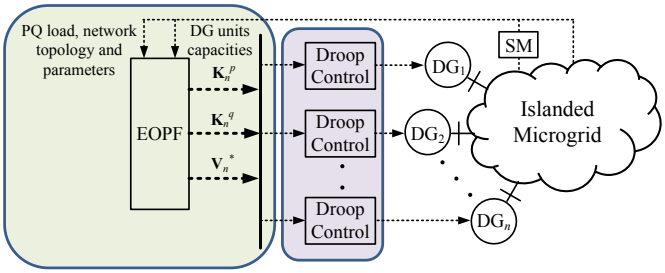

Fig. 3. Hierarchical control scheme.

The proposed hierarchical control includes a primary conventional droop control and a centralized extended optimal power flow control level. The EOPF control level is responsible of computing and sending the droop references K_n^p, K_n^q, and V_n^* for each DG unit primary control as shown in Fig. 3. In order to perform this computation, the information of the microgrid topology, loads and DG units capacities are needed, additionally, a set of constrained nonlinear functions representing the operational goals is required by the optimization method.

It is important to mention that, the online operation of the EOPF control is activated when changes in the load or in the DG units generation capacities occur, in this way, this is an important contribution compared to conventional approaches based on offline optimization schemes. In this work, the changes of generation capacities are performed by random profiles for each DG unit to emulate the changes in the primary energy resources, i.e., wind, solar, among others. Usually, the capacity information is sent from a tertiary control, such as, energy management systems (EMS) [25]; however, this control layer is beyond the scope of this paper but might be added in future works.

In light of the above, a detailed explanation of each stage of the hierarchical control scheme, i.e., primary control, extended power flow and the optimization formulation are addressed below.

A. Primary control: grid-forming droop control

The primary control level is responsible for performing the grid-forming function. This stage is composed of an inner current control loop and an outer voltage control loop which define the control signals for operating the conversion stage as an ideal AC voltage source with a given amplitude $|V|$ and frequency ω [17]. Fig. 4 shows the scheme of the primary controllers working on the dq reference frame. The voltage and frequency references for the voltage sources are derived from the droop control loops, which in turn, receive the droop coefficient (K_n^p, K_n^q) and voltage reference (V_n^*) values from a higher control level (the centralized EOPF control).

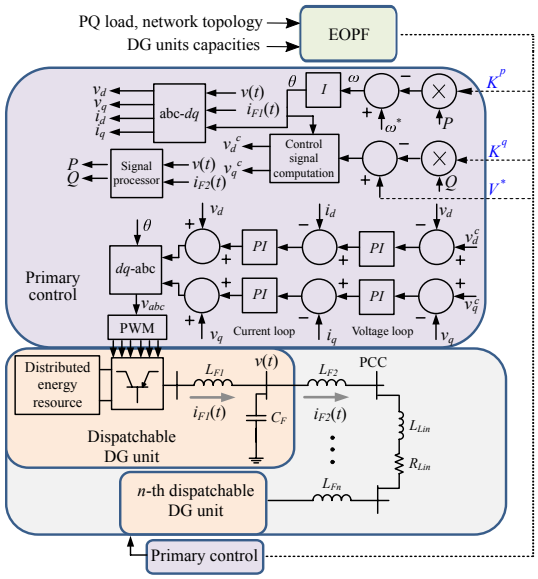

Fig. 4. Basic grid-forming control structure [17].

Due to changing operating circumstances (i.e., the profiles of generation from the DGs and consumption from the loads) the parameters of the droop characteristics, which are defined by the centralized EOPF, should be adjusted for achieving the operational goals of the islanded microgrid. The variations in the parameters of the droop characteristics, and more specifically in the droop coefficients (K_n^p and K_n^q) affect directly the dynamic and steady-state performance of the islanded power system (K_n^p and K_n^q). Because of that, it is important to define the nominal values for the droop coefficient that ensure the stability and proper dynamic behavior of the microgrid. The stability analysis is out of the scope of the paper, however, interested readers may refer to [26], in which a small-signal stability analysis is performed for an islanded microgrid.

Accordingly, Table I summarizes the nominal parameters selected for the case study microgrid as well as the parameters

This article has been accepted for publication in a future issue of this journal, but has not been fully edited. Content may change prior to final publication. Citation information: DOI 10.1109/TPEL.2018.2813980, IEEE Transactions on Power Electronics

of the inner and the outer control loops at the primary control level. Please notice that, for all DG units in this work, for both PI controllers in each loop (current and voltage) the parameters are the same.

TABLE I
PARAMETERS OF THE PRIMARY CONTROL

Parameter	Symbol	Value
$P-\omega$ droop coefficient	K^p	1.25×10^{-5}
$Q-V$ droop coefficient	K^q	1×10^{-3}
Current loop proportional gain	K_{pc}	20
Current loop integral gain	K_{ic}	40
Voltage loop proportional gain	K_{pv}	2.4×10^{-2}
Voltage loop integral gain	K_{iv}	4.5
Commutation frequency	f_c	10 kHz

B. Extended optimal power flow formulation

In electric power systems, the power flow (PF) formulation relies on the well-known power balance equations [27],

$$P_n = \sum_{m=1}^{N} |V_n||V_m||Y_{nm}|cos(\theta_{nm} - \delta_n + \delta_m) \quad for\ n = 1, ..., N \tag{3}$$

$$Q_n = -\sum_{m=1}^{N} |V_n||V_m||Y_{nm}|sin(\theta_{nm} - \delta_n + \delta_m) \quad for\ n = 1, ..., N \tag{4}$$

where $|V_n|$, $|V_m|$, δ_n and δ_m are the magnitudes and phase angles of the n-th and m-th bus voltages, respectively. $|Y_{nm}|$ and θ_{nm} are the magnitude and phase angle of the admittance matrix elements, respectively.

Depending on the topology of the system, the power flow can be formulated using three types of buses: voltage-controlled (PV), load (PQ) and slack [28]. In this way, the active power injected to the system by the PV buses is fixed and known, while the slack bus provides the missing active and reactive power needed by the system.

In islanded droop controlled microgrids, this conventional power flow approach cannot be used in most of the cases because the following reasons [1], [29]: 1) The DG units used in a microgrid have a limited capacity, therefore, a slack bus cannot be assigned for all the operating conditions. 2) The active and reactive power sharing among the DG units depends on the droop characteristics and cannot be pre-specified such as in the conventional power flow. 3) The frequency in an islanded microgrid is changing constantly within a range, while in the conventional power flow, it is considered always fixed.

In regard to the aforementioned, an extra bus classification has to be included to take into account the droop controlled DG units, hereafter called droop buses (DB) [29]. The DB formulation relies on the droop characteristic equations (1) and (2), notice that from these equations the active and reactive power given by the n-th DG unit can be defined as,

$$P_n = \frac{\omega^* - \omega}{K_n^p} \tag{5}$$

$$Q_n = \frac{V_n^* - |V_n|}{K_n^q} \tag{6}$$

therefore, the mismatching equations ΔP_n and ΔQ_n for the n-th DG unit become,

$$\begin{bmatrix} \Delta P_n \\ \Delta Q_n \end{bmatrix} = \begin{bmatrix} P_n - (\frac{\omega^* - \omega}{K_n^p}) \\ Q_n - (\frac{V_n^* - |V_n|}{K_n^q}) \end{bmatrix} \tag{7}$$

Observe that, in (7) the angular frequency is still unknown, therefore, an extra equation related to it has to be included. To overcome this problem, one voltage angle of the DG units is fixed and its active power equation is used as the angular frequency equation as follows [30],

$$\begin{bmatrix} \Delta P_n \\ \Delta Q_n \\ \Delta\omega \end{bmatrix} = \begin{bmatrix} P_n - (\frac{\omega^* - \omega}{K_n^p}) \\ Q_n - (\frac{V_n^* - |V_n|}{K_n^q}) \\ K_n^p P_m - (\omega^* - \omega) \end{bmatrix} \tag{8}$$

where P_m is the active power of the fixed angle bus.

The set of mismatching equations given in (8) completes the power flow formulation of the droop buses, which can be used together with the conventional PV and PQ buses [29]. It is important to notice that the control references K_n^p, K_n^q, and V_n^* that affect the steady-state behavior of the islanded microgrid appear explicitly in the DB formulation, giving the opportunity to use them as variables in the optimization stage.

C. Optimization problem formulation

In order to compute the droop characteristics and voltage reference of each DG unit, an optimization problem has to be solved. The formulation of the problem is specified as follows,

$$min_x\ f(\mathbf{x})\ such\ that \begin{cases} c(\mathbf{x}) \leqslant 0 \\ lb < \mathbf{x} < ub \end{cases} \tag{9}$$

where $\mathbf{x}$ are the variables to optimize, $f(\mathbf{x})$ is the function to minimize, $c(\mathbf{x})$ is a nonlinear function, and lb and ub the lower and upper bound restrictions for the $\mathbf{x}$ values, respectively.

The equations proposed for the optimization formulation are based on three operational goals of the islanded microgrid:

1) The losses of each DG unit is minimized based on their efficiency curves, maximizing the global efficiency of the microgrid.
2) The voltages on the PCCs are maintained close to 1 p.u. through reactive power management.
3) The power injected by the DG units cannot exceed its maximum capacity ($S_n < S_n^{max}$).

The variables to optimize are the droop characteristics and reference values of the primary control K_n^p, K_n^q, and V_n^*. The formulation of each operational goal as a function is explained in detail below.

This article has been accepted for publication in a future issue of this journal, but has not been fully edited. Content may change prior to final publication. Citation information: DOI 10.1109/TPEL.2018.2813980, IEEE Transactions on Power Electronics

1) DG units efficiency function: The efficiency of the DG units is defined based on the relationship between the output power delivered to the microgrid and the input power provided by the primary source [24],

$$\eta_n = \frac{P_n^{out}}{P_n^{in}} \tag{10}$$

this efficiency represents the losses due to conversion, switching of electronic devices, among others. Additionally, the total losses depend on the characteristics of the technology used, the operating point and the switching frequency [24].

In this way, the efficiency of an inverter can be represented graphically for all the load range that it is able to handle. These efficiency curves can be obtained with simulation or experimentally and approximated by a second order function as follows [24],

$$\eta_n = \frac{\alpha_n^1 P_n^{in} + \alpha_n^0}{P_n^{in^2} + \beta_n^1 P_n^{in} + \beta_n^0} \tag{11}$$

where α_n^1, α_n^0, β_n^1 and β_n^0 are the coefficients obtained with the simulation or experimental results of the n-th DG unit.

Hence, in a microgrid composed by n DG units, the global efficiency can be maximized with the reduction of the total losses in the DG units, taking into account that, in the test islanded microgrid the losses in the feeders can be neglected, otherwise, the conductor losses have to be taken into account.

Notice that (11) computes the efficiency using the P_n^{in} but in the power flow method the power computed is P_n^{out}, therefore, substituting $P_n^{in} = P_n^{out}/\eta$, (11) is reformulated and the following quadratic equation is obtained,

$$\eta_n^2 + \eta_n\left(\frac{\beta_n^1}{\beta_n^0}P_n^{out} - \frac{\alpha_n^0}{\beta_n^0}\right) + \frac{P_n^{out^2}}{\beta_n^0} - \frac{\alpha_n^1}{\beta_n^0}P_n^{out} = 0 \tag{12}$$

finally, solving (12) the value of η_n is obtained.

Regarding the aforementioned, this operational goal can be formulated in the optimization problem as follows,

$$\mathbf{F}_\eta = \sum_{n=1}^{N}(P_n^{in} - P_n^{out})^2 \tag{13}$$

where N is the number of DG units. Observe that, if all the DG units are working with an ideal efficiency ($\eta = 1$), the function F_η will be equal to zero, in this way, the minimization of this function will maximize the efficiency of the microgrid. In the case studies presented below, the efficiency parameters used for the DG units were extracted from [24] and are shown in Table II, additionally, the resulting efficiency curves of each DG unit is shown in Fig. 5.

2) PCCs voltage regulation function: Since the power flow solution gives the system bus voltage magnitudes in p.u., the function used to achieve this operational goal can be formulated as follows,

$$\mathbf{F}_V = \sum_{n=1}^{N}(V_{PCCn} - V^{ref})^2 \tag{14}$$

TABLE II
PARAMETERS OF THE EFFICIENCY CURVES

Curve	α_n^1	α_n^0	β_n^1	β_n^0
η_1	7.317	-0.081	5.85	0.77
η_2	5.072	-0.037	4.4	0.18
η_3	8.249	-0.113	5.45	2.15

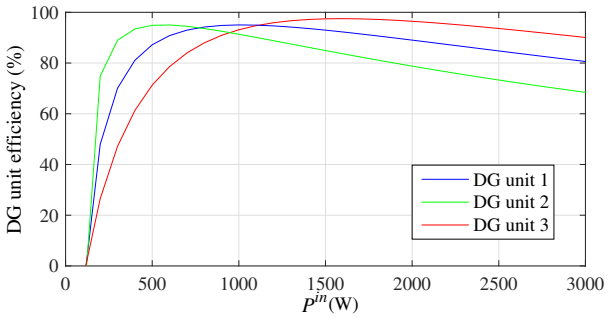

Fig. 5. Efficiency curves of the DG units [24].

notice that if the magnitudes of voltages V_{PCCn} are equal to the voltage reference $V^{ref} = 1$ p.u., the summation of the function will be equal to zero. It is important to note that the voltage in the different PCCs is related to the reactive power as shown in (2), in this way, the voltage is regulated with reactive power management (selecting K_n^q and V_n^*), without the need of an extra control loop.

3) Power restriction: The power restriction is included in the optimization problem as an inequality function in $c(\mathbf{x}) \leqslant 0$ as,

$$c(\mathbf{x}) = \mathbf{S}_n - \mathbf{S}_n^{max} \leqslant 0, \quad for\ n = 1, ..., N \tag{15}$$

while this inequality is true, the power injected by the n-th DG unit will not exceed its capacity.

Regarding the aforementioned, the optimization problem is built as a sum of each operational goal function, subject to the capacity restriction as follows,

$$\begin{aligned} &min_x\ f(\mathbf{x}) = \alpha\mathbf{F}_\eta + \beta\mathbf{F}_V \\ &Subject\ to \quad \mathbf{S} - \mathbf{S}^{max} \leqslant 0 \end{aligned} \tag{16}$$

where α and β are weights, the solution of this problem gives the control references $\mathbf{K}^p = [K_1^p, ..., K_n^p]$, $\mathbf{K}^q = [K_1^q, ..., K_n^q]$, and $\mathbf{V}^* = [V_1^*, ..., V_n^*]$. In order to have a better understating of the optimization, in Fig. 6 a flowchart of the EOPF is shown. Note that, since the optimal formulation is performed through the power flow, other operational goals can be added easily for different MG topologies that might need specific features, such as, losses minimization [31] (for both active and reactive power), cost minimization [32], among others.

It is important to mention that, in this work the problem is solved using the *fmincon* optimization tool of MATLAB, which for the test system used, has a good performance in terms of computation time, i.e., 1.58 seconds per optimization

This article has been accepted for publication in a future issue of this journal, but has not been fully edited. Content may change prior to final publication. Citation information: DOI 10.1109/TPEL.2018.2813980, IEEE Transactions on Power Electronics

with an error tolerance of 1×10^{-6}; however, other optimization techniques can be used to solve the minimization problem shown in (16).

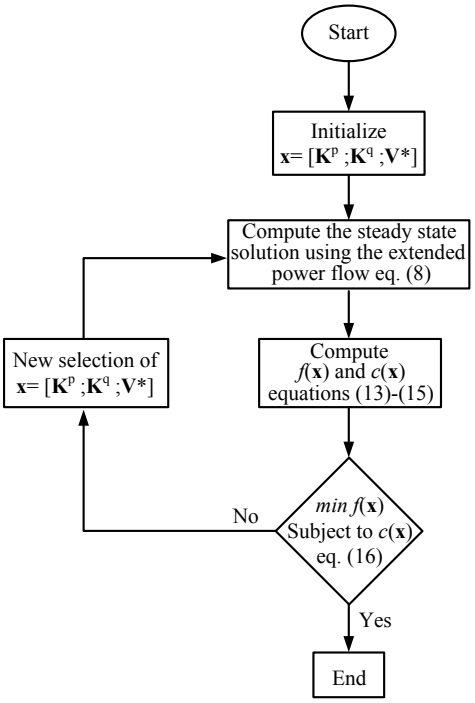

Fig. 6. Control optimization flowchart.

III. Test System and Laboratory Implementation

Figure 7 shows the single line diagram of the three-phase microgrid used as test system. It includes three dispatchable DG units with LC-filters connected to each PCC through a RL feeder impedance, two fixed R loads wye-connected to PCC_1 and PCC_3, and a variable PQ load connected to PCC_2. Additionally, the PCCs are connected through RL lines and the variable load is measured by a smart meter (SM).

TABLE III
Parameters of the Microgrid

Parameter	Symbol	Value
Nominal voltage	V_{L-L}^{RMS}	400 V
Nominal frequency	f^*	50 Hz
Nominal capacity	S^{max}	2.5 kVA
Nominal DC voltage	V_{DC}	650 V
Filter resistance	R_{11}, R_{12}, R_{21}, R_{22}, R_{31}, R_{32}	0.1 Ω
Filter inductance	L_{11}, L_{12}, L_{21}, L_{22}, L_{31}, L_{32}	1.25 mH
Filter capacitance	C_{11}, C_{21}, C_{31}	27 μF
Feeder resistance	R_{f1}, R_{f2}, R_{f3}	0.1 Ω
Feeder inductance	L_{f1}, L_{f2}, L_{f3}	1.25 mH
Line resistance	R_{Lin1}, R_{Lin2}	0.45 Ω
Line inductance	L_{Lin1}, L_{Lin2}	1.45 mH
Wye-resistance load	R_{L1}, R_{L2}	119 Ω

The primary control is modeled and included in a real time platform (dSPACE 1006), while the EOPF stage is

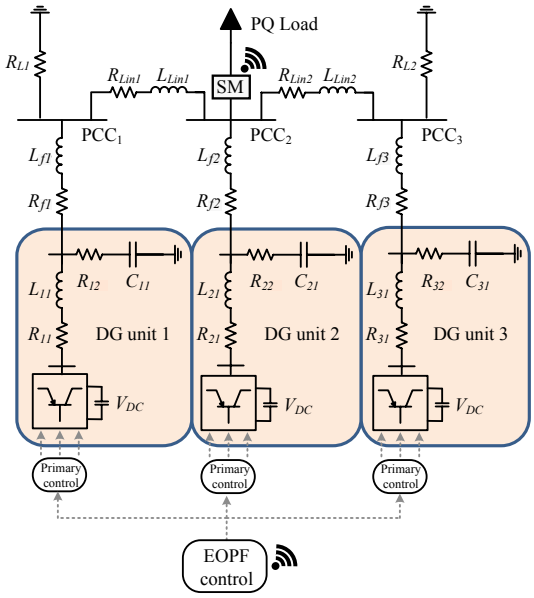

Fig. 7. Single line diagram of the three-phase microgrid test system.

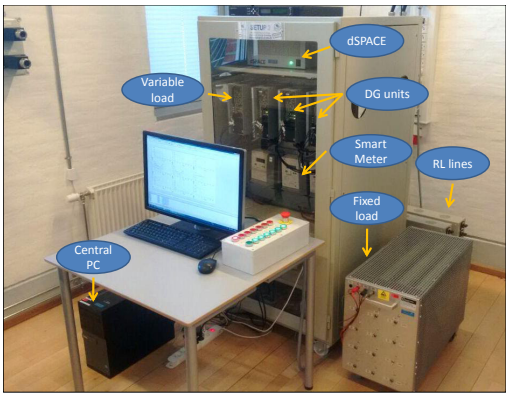

Fig. 8. Laboratory implementation of the islanded microgrid.

incorporated in a central computer (CPC) which sends and receives information to the dSPACE via ethernet using a User Datagram Protocol (UDP) [33].

For the measurement of the variable load, a Kamstrup Smart Meter is used. The SM is connected to a central data base, which is responsible of handle and synchronize the information sent by one or a cluster of SMs [34]. The communication implemented in the laboratory is the TCP/IP connection, which allows an easy incorporation of several SMs working over the same network structure [34].

The communication between the dSPACE and the CPC is performed through an interface using the professional software LabVIEW [35]. The SM is constantly sending the measures of the variable load to the central data base, which in turn sends the information to the CPC through the LabVIEW interface; if there is a change of load with respect to the last measurement received, it calls the MATLAB software to perform the optimization process. The CPC sends the computed control parameters to the dSPACE and it uses this

This article has been accepted for publication in a future issue of this journal, but has not been fully edited. Content may change prior to final publication. Citation information: DOI 10.1109/TPEL.2018.2813980, IEEE Transactions on Power Electronics

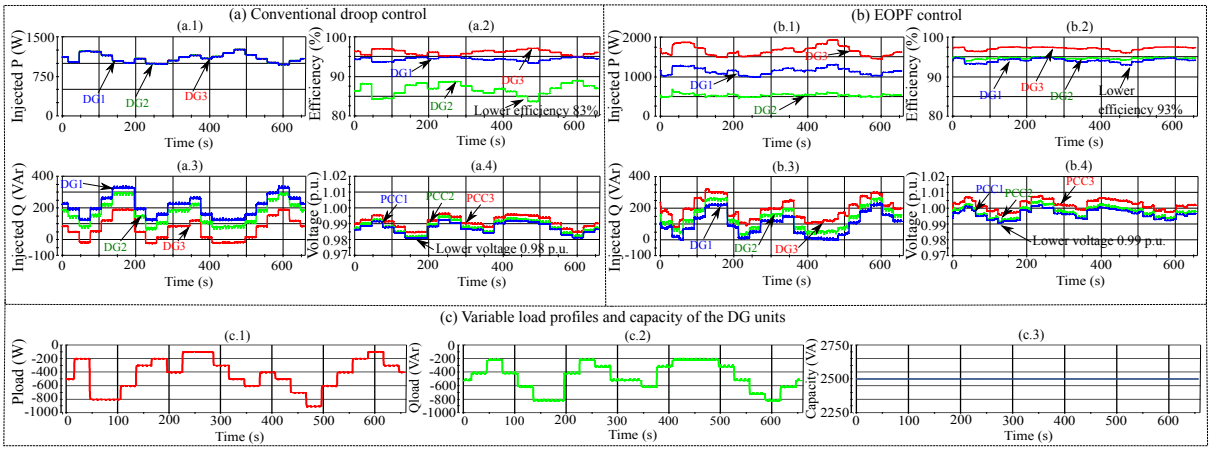

Fig. 9. Case I: (a) conventional droop control response, (b) EOPF control response and (c) load and capacities profiles.

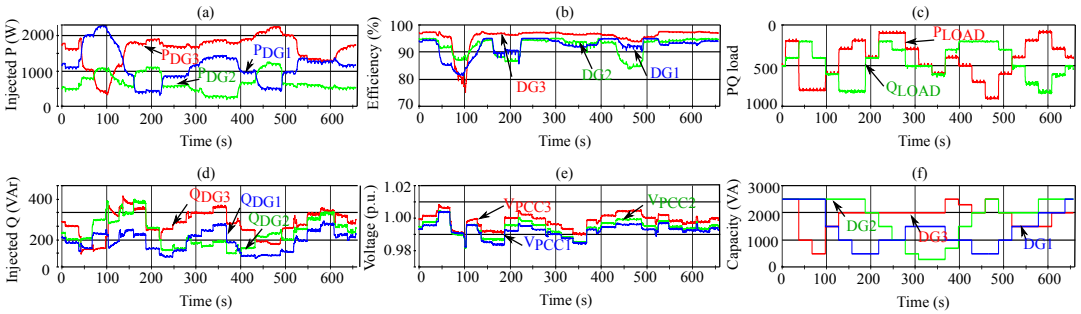

Fig. 10. Case II: Hierarchical control scheme response under load and capacity profiles.

information in the DG units primary control.

The parameters of the test microgrid are shown in Table III, they were obtained from the real values of the laboratory implementation, which was made in the Microgrid Research Laboratory in Aalborg University [33] with an online architecture as can be seen in Fig. 8.

IV. Case Studies

To validate the proposed hierarchical scheme, in this section two case studies of the islanded MG under different practical operational conditions are presented. In the first case study, the load connected to the PCC_2 is changing following a load profile. The load profile has 24 changes made every 30 seconds, emulating a load variation every hour in a day.

In a practical MG based on variable energy resources (solar, wind, etc.), the power that can be injected by the DG units is not always constant. In this way, power capacity profiles are included for each DG unit in the second case study, emulating the variation in the primary energy resources and to take into account this effect in the performance of the control.

In both cases, the control of the islanded microgrid is performed online using the hierarchical control and the measurements of the SM; however, in the first case study, the experiment is also conducted using only the conventional droop control to show the advantages of the proposed control scheme.

A. Case I: Load profile

The results obtained in this case for both, conventional droop control and the proposed hierarchical control, are shown in Fig. 9(a) and 9(b), respectively. Besides, the load profiles for active and reactive power and the capacities for the DG units are shown in Fig. 9(c).

Notice that, using the conventional droop control, due to the control references K_n^p, K_n^q, and V_n^* are the same for all the DG units, the active and reactive power shared among the units is very similar (Fig. 9(a.1) and 9(a.3)). Consequently, the efficiency of each DG unit is not taken into account in the operation of the microgrid as can be seen in Fig. 9(a.2), where in the worst case, drops up to 83 %. Additionally, observe that the PCCs voltage are always below 1 p.u., which in the worst case, drops up to 0.98 p.u. when the reactive power load is incremented.

On the other hand, using the EOPF control, observe in Fig. 9(b.1) that in order to get a better efficiency, each DG unit shares a different amount of active power depending on its efficiency curve. Notice Fig. 9(b.2) that, in the worst case, the efficiency drops up to 93 %. Additionally, in this case, the PCCs voltage are maintained close to 1 p.u., which in the worst case, drops up to 0.99 p.u.

Note that, the desired operational goals proposed in Section IV are achieved taking into account random load variations and measurements from a practical Smart Meter. In this case,

compared with the conventional droop control, the efficiency is improved 10 % and the voltage is regulated closer to the desired nominal value.

B. Case II: Load and capacity profiles

The results obtained for the second case study are shown in Fig. 10. The load and capacity profiles are shown in Figures 10(c) and 10(f), respectively. Notice that the capacity of the DG units changes constantly causing a variation of the active and reactive powers injected by the DG units, because of the restriction of the capacity limits included in the EOPF control.

Despite the changes of active and reactive power due to the capacity restriction, the PCCs voltage are kept close to the nominal voltage value, having in the worst case a drop up to 0.98 p.u. On the other hand, observe in Fig. 10(b) that the control tries to maximize the efficiency but the capacity restrictions limit the control optimization, i.e., if the n-th DG unit best efficiency is reached at 1.5 kW but the power capacity drops to 1 kW, it will not be able to reach its best efficiency.

The results obtained in the case studies show that the proposed hierarchical control is a reliable online scheme capable to manage different operational conditions, such as, random load and capacity profiles, and including practical devices such as the SM. On the other hand, the optimal extended power flow, which is based on the conventional formulation, has the advantage that any change in the microgrid topology can be updated in an easy and straightforward manner, besides, the operational goals can be also changed or improved depending on the operational needs of the islanded microgrid.

V. Conclusion

In this paper, the application of a hierarchical control scheme with a primary droop control and a central extended optimal power flow for the online operation of islanded microgrids is presented. Two case studies of an islanded microgrid were implemented in the laboratory and online tested, considering three different PCCs, frequency variations, transmission lines impedance, efficiency characteristic curves of each DG unit, random capacities of the DG units and load variations. The control scheme optimally tuned, in an online manner, the droop characteristics and voltage control parameters to perform active and reactive power management to achieve voltage regulation, maximum efficiency, while maintaining the capacity constraints of each DG unit.

The results obtained in the case studies revealed the applicability, advantages and drawbacks of the control scheme. It was shown that even with random PQ load and capacity variations, the proposed control, working online, regulates the voltage magnitude of the different PCCs and maximizes the efficiency of the DG units. On the other hand, notice that the computation time for the optimization method in the hierarchical control is less than 2 seconds which, in tertiary control schemes, is a good time for power management as seen in the results. Therefore, it is shown that the application of power flow based hierarchical control schemes contributes to the system to achieve optimized operating points in a reliable way. Notice that, the case studies reported in this paper consider always enough generation capacity for supplying the local loads; however, in future works will consider lower generation capacities than the total load and energy storage systems in grid-connected and islanded microgrids.

References

[1] C. Li, S. K. Chaudhary, J. C. Vasquez, and J. M. Guerrero, "Power flow analysis algorithm for islanded lv microgrids including distributed generator units with droop control and virtual impedance loop," in *2014 IEEE Applied Power Electronics Conference and Exposition - APEC 2014*, March 2014, pp. 3181–3185.

[2] J. Schiffer, D. Zonetti, R. Ortega, A. Stankovic, T. Sezi, and J. Raisch, "A survey on modeling of microgrids - from fundamental physics to phasors and voltage sources," *ArXiv*, May 2015.

[3] K. Balamurugan and D. Srinivasan, "Review of power flow studies on distribution network with distributed generation," in *Power Electronics and Drive Systems (PEDS), 2011 IEEE Ninth International Conference on*, Dec 2011, pp. 411–417.

[4] A. Bidram, F. L. Lewis, and A. Davoudi, "Distributed control systems for small-scale power networks: Using multiagent cooperative control theory," *IEEE Control Systems*, vol. 34, no. 6, pp. 56–77, Dec 2014.

[5] F. Marra and G. Yang, "Chapter 10 - decentralized energy storage in residential feeders with photovoltaics," in *Energy Storage for Smart Grids*, P. D. Lu, Ed. Boston: Academic Press, 2015, pp. 277 – 294.

[6] T. L. Vandoorn, J. C. Vasquez, J. D. Kooning, J. M. Guerrero, and L. Vandevelde, "Microgrids: Hierarchical control and an overview of the control and reserve management strategies," *IEEE Industrial Electronics Magazine*, vol. 7, no. 4, pp. 42–55, Dec 2013.

[7] J. M. Guerrero, J. C. Vsquez, and R. Teodorescu, "Hierarchical control of droop-controlled dc and ac microgrids: a general approach towards standardization," in *2009 35th Annual Conference of IEEE Industrial Electronics*, Nov 2009, pp. 4305–4310.

[8] S. Chowdhury and P. Crossley, *Microgrids and Active Distribution Networks*, ser. IET renewable energy series. Institution of Engineering and Technology, 2009.

[9] D. E. Olivares, A. Mehrizi-Sani, A. H. Etemadi, C. A. Caizares, R. Iravani, M. Kazerani, A. H. Hajimiragha, O. Gomis-Bellmunt, M. Saeedifard, R. Palma-Behnke, G. A. Jimnez-Estvez, and N. D. Hatziargyriou, "Trends in microgrid control," *IEEE Transactions on Smart Grid*, vol. 5, no. 4, pp. 1905–1919, July 2014.

[10] R. A. Mohr, R. Moreno, and H. Rudnick, "Insertion of distributed generation into rural feeders," in *2009 CIGRE/IEEE PES Joint Symposium Integration of Wide-Scale Renewable Resources Into the Power Delivery System*, July 2009, pp. 1–10.

[11] R. Lasseter, A. Akhil, C. Marnay, J. Stevens, J. Dagle, R. Guttromson, S. A. Meliopoulous, R. Yinger, and J. Eto, "The CERTS MicroGrid Concept - White Paper on Integration of Distributed Energy Resources," U.S. Department of Energy, Tech. Rep., Apr. 2002.

[12] L. Zhang, H. Xin, Z. Wang, and D. Gan, "A decentralized quasi-hierarchical control scheme for droop-controlled ac island microgrids," in *2016 IEEE Power and Energy Society General Meeting (PESGM)*, July 2016, pp. 1–5.

[13] L. Che, M. Shahidehpour, A. Alabdulwahab, and Y. Al-Turki, "Hierarchical coordination of a community microgrid with ac and dc microgrids," *IEEE Transactions on Smart Grid*, vol. 6, no. 6, pp. 3042–3051, Nov 2015.

[14] E. R. Sanseverino, N. N. Quang, M. L. D. Silvestre, J. M. Guerrero, and C. Li, "Optimal power flow in three-phase islanded microgrids with inverter interfaced units," *Electric Power Systems Research*, vol. 123, no. Supplement C, pp. 48 – 56, 2015.

[15] E. R. Sanseverino, N. Q. Nguyen, M. L. D. Silvestre, G. Zizzo, F. de Bosio, and Q. T. T. Tran, "Frequency constrained optimal power flow based on glow-worm swarm optimization in islanded microgrids," in *2015 AEIT International Annual Conference (AEIT)*, Oct 2015, pp. 1–6.

[16] C. Deckmyn, T. Vandoorn, J. V. de Vyver, J. Desmet, and L. Vandevelde, "A microgrid multilayer control concept for optimal power scheduling and voltage control," *IEEE Transactions on Smart Grid*, 2017.

[17] J. Rocabert, A. Luna, F. Blaabjerg, and P. Rodrguez, "Control of power converters in ac microgrids," *IEEE Transactions on Power Electronics*, vol. 27, no. 11, pp. 4734–4749, Nov 2012.

[18] J. A. P. Lopes, C. L. Moreira, and A. G. Madureira, "Defining control strategies for microgrids islanded operation," *IEEE Transactions on Power Systems*, vol. 21, no. 2, pp. 916–924, May 2006.

[19] J. Guerrero, L. Garcia De Vicuna, J. Matas, M. Castilla, and J. Miret, "A wireless controller to enhance dynamic performance of parallel inverters in distributed generation systems," *IEEE Transactions on Power Electronics*, vol. 19, no. 5, pp. 1205–1213, Sept 2004.

[20] R. A. Mohr, R. Moreno, and H. Rudnick, "Insertion of distributed generation into rural feeders," in *2009 CIGRE/IEEE PES Joint Symposium Integration of Wide-Scale Renewable Resources Into the Power Delivery System*, July 2009, pp. 1–10.

[21] j. zhou, S. Kim, H. Zhang, Q. Sun, and R. Han, "Consensus-based distributed control for accurate reactive, harmonic and imbalance power sharing in microgrids," *IEEE Transactions on Smart Grid*, vol. PP, no. 99, pp. 1–1, 2016.

[22] Y. Zhu, F. Zhuo, F. Wang, B. Liu, and Y. Zhao, "A wireless load sharing strategy for islanded microgrid based on feeder current sensing," *IEEE Transactions on Power Electronics*, vol. 30, no. 12, pp. 6706–6719, Dec 2015.

[23] H. Zhang, S. Kim, Q. Sun, and J. Zhou, "Distributed adaptive virtual impedance control for accurate reactive power sharing based on consensus control in microgrids," *IEEE Transactions on Smart Grid*, vol. PP, no. 99, pp. 1–13, 2016.

[24] F. H. Dupont, J. Zaragoza, C. Rech, and J. R. Pinheiro, "A new method to improve the total efficiency of parallel converters," in *2013 Brazilian Power Electronics Conference*, Oct 2013, pp. 210–215.

[25] A. C. Luna, N. L. Diaz, M. Graells, J. C. Vasquez, and J. M. Guerrero, "Mixed-integer-linear-programming-based energy management system for hybrid pv-wind-battery microgrids: Modeling, design, and experimental verification," *IEEE Transactions on Power Electronics*, vol. 32, no. 4, pp. 2769–2783, April 2017.

[26] N. L. Díaz, E. A. Coelho, J. C. Vasquez, and J. M. Guerrero, "Stability analysis for isolated ac microgrids based on pv-active generators," in *2015 IEEE Energy Conversion Congress and Exposition (ECCE)*, Sept 2015, pp. 4214–4221.

[27] W. Stevenson and J. Grainger, *Power System Analysis*, ser. McGraw-Hill series in electrical and computer engineering: Power and energy. McGraw-Hill Education (India) Pvt Limited, 2003.

[28] H. Saadat, *Power System Analysis*, ser. McGraw-Hill series in electrical and computer engineering. McGraw-Hill, 2002.

[29] M. M. A. Abdelaziz, H. E. Farag, E. F. El-Saadany, and Y. A. R. I. Mohamed, "A novel and generalized three-phase power flow algorithm for islanded microgrids using a newton trust region method," *IEEE Transactions on Power Systems*, vol. 28, no. 1, pp. 190–201, Feb 2013.

[30] C. Li, S. K. Chaudhary, M. Savaghebi, J. C. Vasquez, and J. M. Guerrero, "Power flow analysis for low-voltage ac and dc microgrids considering droop control and virtual impedance," *IEEE Transactions on Smart Grid*, 2016.

[31] M. Han, D. Xu, and L. Wan, "Hierarchical optimal power flow control for loss minimization in hybrid multi-terminal hvdc transmission system," *CSEE Journal of Power and Energy Systems*, vol. 2, no. 1, pp. 40–46, March 2016.

[32] K. R. C. Mamandur and R. D. Chenoweth, "Optimal control of reactive power flow for improvements in voltage profiles and for real power loss minimization," *IEEE Transactions on Power Apparatus and Systems*, vol. PAS-100, no. 7, pp. 3185–3194, July 1981.

[33] L. Meng, A. Luna, E. R. Daz, B. Sun, T. Dragicevic, M. Savaghebi, J. C. Vasquez, J. M. Guerrero, M. Graells, and F. Andrade, "Flexible system integration and advanced hierarchical control architectures in the microgrid research laboratory of aalborg university," *IEEE Transactions on Industry Applications*, vol. 52, no. 2, pp. 1736–1749, March 2016.

[34] E. J. Palacios-Garca, Y. Guan, M. Savaghebi, J. C. Vsquez, J. M. Guerrero, A. Moreno-Munoz, and B. S. Ipsen, "Smart metering system for microgrids," in *IECON 2015 - 41st Annual Conference of the IEEE Industrial Electronics Society*, Nov 2015, pp. 003 289–003 294.

[35] C. Elliott, V. Vijayakumar, W. Zink, and R. Hansen, "National instruments labview: A programming environment for laboratory automation and measurement," *JALA: Journal of the Association for Laboratory Automation*, vol. 12, no. 1, pp. 17–24, 2007.